

Article

A Fifteen Year Record of Global Natural Gas Flaring Derived from Satellite Data

Christopher D. Elvidge ^{1,*}, Daniel Ziskin ², Kimberly E. Baugh ², Benjamin T. Tuttle ^{2,3},
Tilottama Ghosh ^{2,3}, Dee W. Pack ⁴, Edward H. Erwin ¹ and Mikhail Zhizhin ⁵

¹ Earth Observation Group, Solar and Terrestrial Division, NOAA National Geophysical Data Center, 325 Broadway, Boulder, CO 80305, USA; E-Mail: edward.h.erwin@noaa.gov

² Cooperative Institute for Research in Environmental Science, University of Colorado, Boulder, CO 80303, USA; E-Mails: daniel.ziskin@noaa.gov (D.Z.); kim.baugh@noaa.gov (K.E.B.); ben.tuttle@noaa.gov (B.T.T.); tilottama.ghosh@noaa.gov (T.G.)

³ Department of Geography, University of Denver, Denver, CO, USA

⁴ The Aerospace Corporation, El Segundo, CA, USA; E-Mail: dee.w.pack@aerospace.org

⁵ Space Research Institute, Russian Academy of Science, Moscow, Russia;
E-Mail: jjn@wdcb.ru

* Author to whom correspondence should be addressed; E-Mail: chris.elvidge@noaa.gov;
Tel.: +1-303-497-6121; Fax: +1-303-497-6513

Received: 3 July 2009; in revised form: 30 July 2009 / Accepted: 5 August 2009 /

Published: 7 August 2009

Abstract: We have produced annual estimates of national and global gas flaring and gas flaring efficiency from 1994 through 2008 using low light imaging data acquired by the Defense Meteorological Satellite Program (DMSP). Gas flaring is a widely used practice for the disposal of associated gas in oil production and processing facilities where there is insufficient infrastructure for utilization of the gas (primarily methane). Improved utilization of the gas is key to reducing global carbon emissions to the atmosphere. The DMSP estimates of flared gas volume are based on a calibration developed with a pooled set of reported national gas flaring volumes and data from individual flares. Flaring efficiency was calculated as the volume of flared gas per barrel of crude oil produced. Global gas flaring has remained largely stable over the past fifteen years, in the range of 140 to 170 billion cubic meters (BCM). Global flaring efficiency was in the seven to eight cubic meters per barrel from 1994 to 2005 and declined to 5.6 m³ per barrel by 2008. The 2008 gas flaring estimate of 139 BCM represents 21% of the natural gas consumption

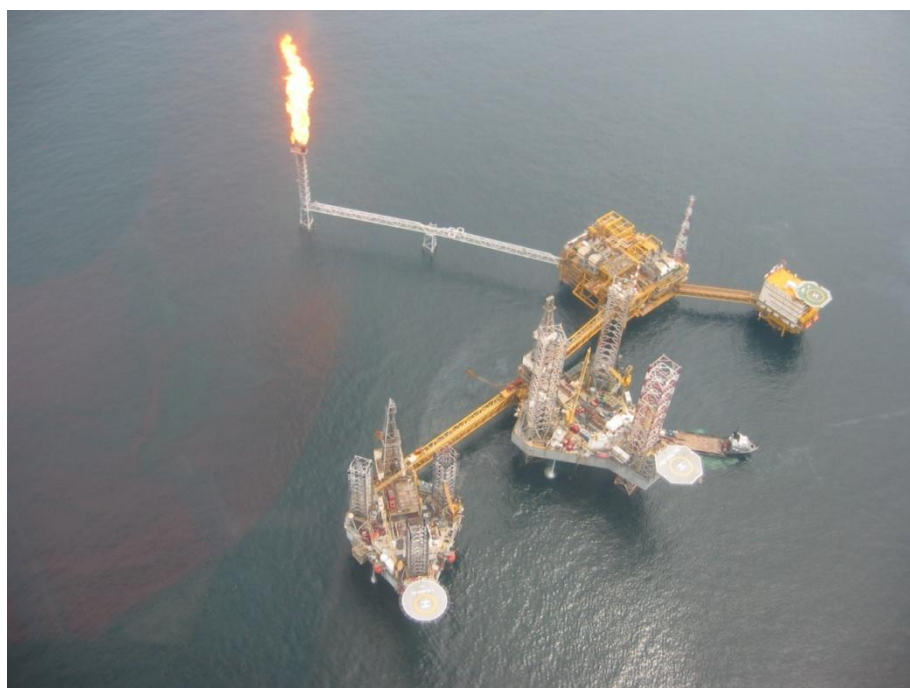
of the USA with a potential retail market value of \$68 billion. The 2008 flaring added more than 278 million metric tons of carbon dioxide equivalent (CO₂e) into the atmosphere. The DMSP estimated gas flaring volumes indicate that global gas flaring has declined by 19% since 2005, led by gas flaring reductions in Russia and Nigeria, the two countries with the highest gas flaring levels. The flaring efficiency of both Russia and Nigeria improved from 2005 to 2008, suggesting that the reductions in gas flaring are likely the result of either improved utilization of the gas, reinjection, or direct venting of gas into the atmosphere, although the effect of uncertainties in the satellite data cannot be ruled out. It is anticipated that the capability to estimate gas flaring volumes based on satellite data will spur improved utilization of gas that was simply burnt as waste in previous years.

Keywords: gas flaring; carbon emissions; nighttime lights

1. Introduction

We present the first consistently derived estimates of national and global gas flaring volumes. The estimates span a fifteen year time period (1994–2008) and were derived from satellite data. Gas flaring is widely used to dispose of dissolved natural gas present in petroleum in production and processing facilities where there is no infrastructure to make use of the gas (see Figure 1). The gas emerges from crude oil when it is brought to the surface and is separated from the oil prior to transport. Information on the spatial and temporal distribution of gas flaring has not been available previously due the sparse and unverifiable nature of the reporting done by countries and petroleum companies.

Figure 1. Most gas flaring occurs at remote petroleum production or processing facilities, many of which are offshore.



Gas flaring is responsible for a vast amount of both wasted energy and greenhouse gas emissions. Over the fifteen year record that was observed, we estimate that 2.4×10^{12} m³ of gas was flared—creating 5,000 Mt (mega metric tons) of CO₂e or roughly 70% of the total annual greenhouse gas emissions of the United States in 2007.

The World Bank in cooperation with the Government of Norway launched a Global Gas Flaring Reduction (GGFR) initiative at the World Summit on Sustainable Development in August, 2002. The ultimate goal of the GGFR is the elimination of most gas flaring and venting. The GGFR is a public-private partnership with participation from governments of oil-producing countries, state-owned companies and major international oil companies. The GGFR identifies areas where gas flaring occurs and works with the countries and companies to promote regulatory frameworks and infrastructure investment to bring flared gas to markets. A growing array of technologies to capture and make use of the gas have emerged, ranging from transport to markets as gas using pipelines, reinjection to boost oil production, conversion to liquids that can be more readily transported, and use on site. GGFR country partners include the countries of Algeria (Sonatrach), Angola (Sonangol), Azerbaijan, Cameroon, Ecuador, Equatorial Guinea, Gabon, Indonesia, Kazakhstan, Khanty-Mansiysk (Russian Federation), Nigeria, Norway, Qatar, United States, and Uzbekistan. Participating oil companies include BP, Chevron, ConocoPhillips, ENI, ExxonMobil, Marathon Oil, Shell, StatoilHydro, and TOTAL. OPEC and the World Bank Group are also GGFR partners. Donor countries are Canada, European Union, France, Norway, UK Foreign Commonwealth Office, and the United States.

Because flaring is used as a disposal process and typically occurs at remote locations, there are not good records on the volume of flared gas. There are a large number of countries with no publicly reported gas flaring volumes and it is widely agreed that there is substantial uncertainty regarding the magnitude of gas flaring. Through the GGFR a substantial amount of effort and international attention has been focused on the reduction of gas flaring since 2002. Without independent data sources and methods for estimating gas flaring, how can progress towards the elimination of gas flaring be assessed? Is it possible to monitor gas flaring to identify areas where gas flaring has been reduced over time? Is it possible to independently estimate gas flaring volumes?

To address these questions, in a project sponsored by the GGFR Partnership, we have investigated the use of earth observation satellite data for the detection of gas flaring and estimation of gas flaring volumes. Because of their ability to collect consistent data repeatedly over large areas satellite sensors would appear to have good potential for observing gas flaring activity. However, none of the currently available earth observation sensors have been designed and flown specifically for the observation of gas flaring. In reviewing the available sources we found several satellite systems have a capability to detect gas flares based on the radiative emissions from the flames. Given the wide spatial distribution and possibility that gas flaring activity fluctuates over time, particular attention has to be given to sensors that collect data globally on a frequent basis and have a capability to readily detect gas flaring. The other factor to consider is the length of the archived record and the prospects for continuity of the observations. Based on these considerations we have initially worked with the low light imaging data from the U.S. Air Force Defense Meteorological Satellite Program (DMSP) Operational Linescan System (OLS). The detection of gas flares in OLS data was first described in the early 1970's [1]. A digital archive of OLS data extends from 1992 to the present and the observations are expected to continue into the coming decades from DMSP and the U.S. National Polar Orbiting Environmental

Satellite System (NPOESS). In this paper we present annual results from the DMSP archive spanning 1994 through 2008.

2. Experimental Section

2.1. DMSP Nighttime Lights

The DMSP OLS was designed to collect global cloud imagery using a pair of broad spectral bands placed in the visible and thermal. The DMSP satellites are flown in polar orbits and each collects fourteen orbits per day. With a 3,000 km swath width, each OLS is capable of collecting a complete set of images of the Earth twice a day. At night the visible band signal is intensified with a photomultiplier tube (PMT) to enable the detection of moonlit clouds. The boost in gain enables the detection of lights present at the Earth's surface. Most of the lights are from human settlements (cities and towns) and ephemeral fires. Gas flares are also detected and can easily be identified when they are offshore or in isolated areas not impacted by urban lighting.

NGDC serves as the long term archive for DMSP, with data extending from 1992 to the present. The archive is organized as individual orbits which are labeled to indicate the year, month, date and start time. For this project the individual orbits were processed with automatic algorithms that identify image features (such as lights and clouds) and the quality of the nighttime data [2,3]. The following criteria were used to identify the best nighttime lights data for compositing:

1. Center half of orbital swath (best geolocation, reduced noise, and sharpest features).
2. No sunlight present.
3. No moonlight present.
4. No solar glare contamination.
5. Cloud-free (based on thermal detection of clouds).
6. No contamination from auroral emissions.

Nighttime image data from individual orbits that meet the above criteria are added into a global latitude-longitude grid (Platte Carree projection) having a resolution of 30 arc seconds. This grid cell size is approximately a square kilometer at the equator. The total number of coverages and number of cloud-free coverages are also tallied. In the typical annual cloud-free composite most areas have twenty to a hundred cloud-free observations (Figure 2), providing a temporal sampling of activities such as gas flaring. Before being used in the gas flaring analysis each composite is converted into a Mollweide one km² equal area grid (see Figure 3).

The nighttime lights product used in the gas flaring analysis is the average visible band digital number (DN) of cloud-free light detections multiplied by the percent frequency of light detection. The inclusion of the percent frequency of detection term normalizes the resulting digital values for variations in the persistence of flaring. For instance the value for a gas flare only detected half the time is discounted by 50%. This style of nighttime lights is referred to as the "lights index". The gas flaring analyses are conducted on the lights index images that have been converted to one kilometer square equal area grids (Mollweide projection, see Figure 3). The "sum of lights index" used to analyze the magnitude of gas flaring is derived by summing the lights index values of 8.0 or greater for all the

one km² grid cells identified as gas flares. Grid cells having lights index values of less than eight are ignored to eliminate background noise present in the products. Analysis of the actual value of the threshold showed no qualitative differences as the threshold was adjusted.

Figure 2. Tally of cloud-free coverages from DMSP satellite F16 for the year 2004.

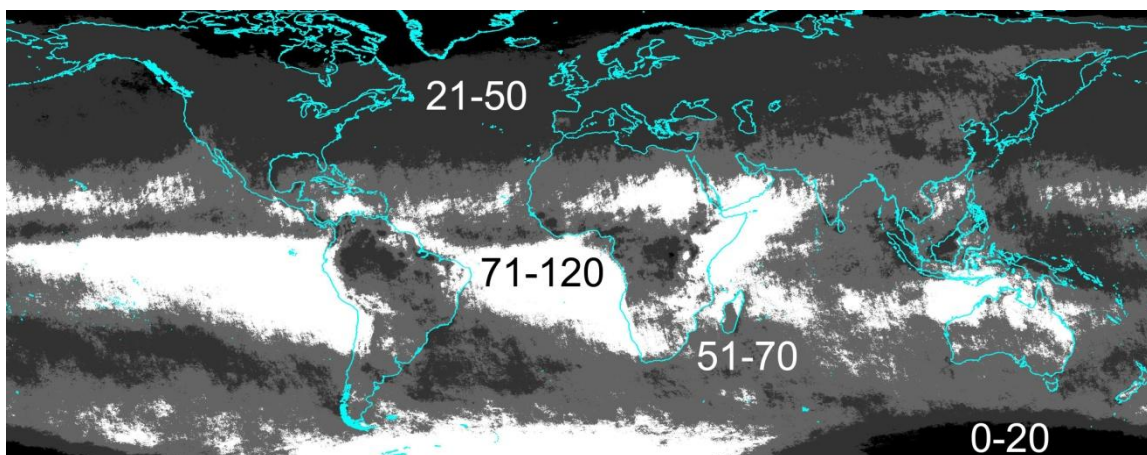
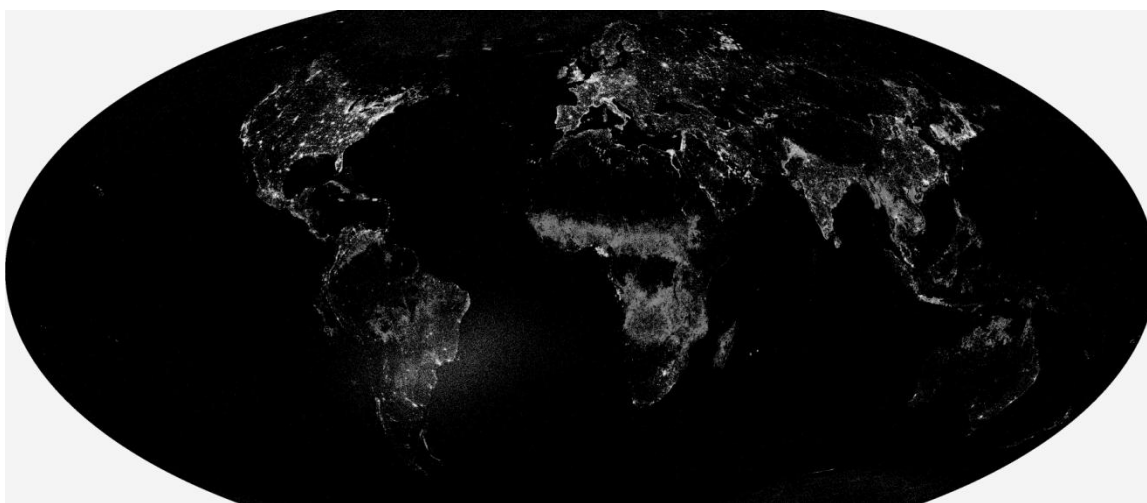


Figure 3. Mollweide equal area projection version of the DMSP nighttime lights derived from satellite F16 for year 2004.



A set of annual composites were processed for each satellite that collected nighttime lights data from 1994 through 2008 (see Table 1). Each satellite is designated with a flight number, such as F12 for DMSP satellite number 12. Data for the archive generally begins within a few weeks after launch. Over time the satellites/sensors age and eventually are no longer able to produce data. The degradation is typically gradual enough that a replacement satellite can be deployed to ensure continuity. Thus in most years two satellites collected data and two separate composites were produced. The annual composites were used to estimate gas flaring volumes for each year from 1994 through 2008. The earlier part of the DMSP archive (1992–1994) was not found to be consistent with the later part of the

record. It may be possible to extend the record back to 1992 if current efforts to create an absolute calibration succeed.

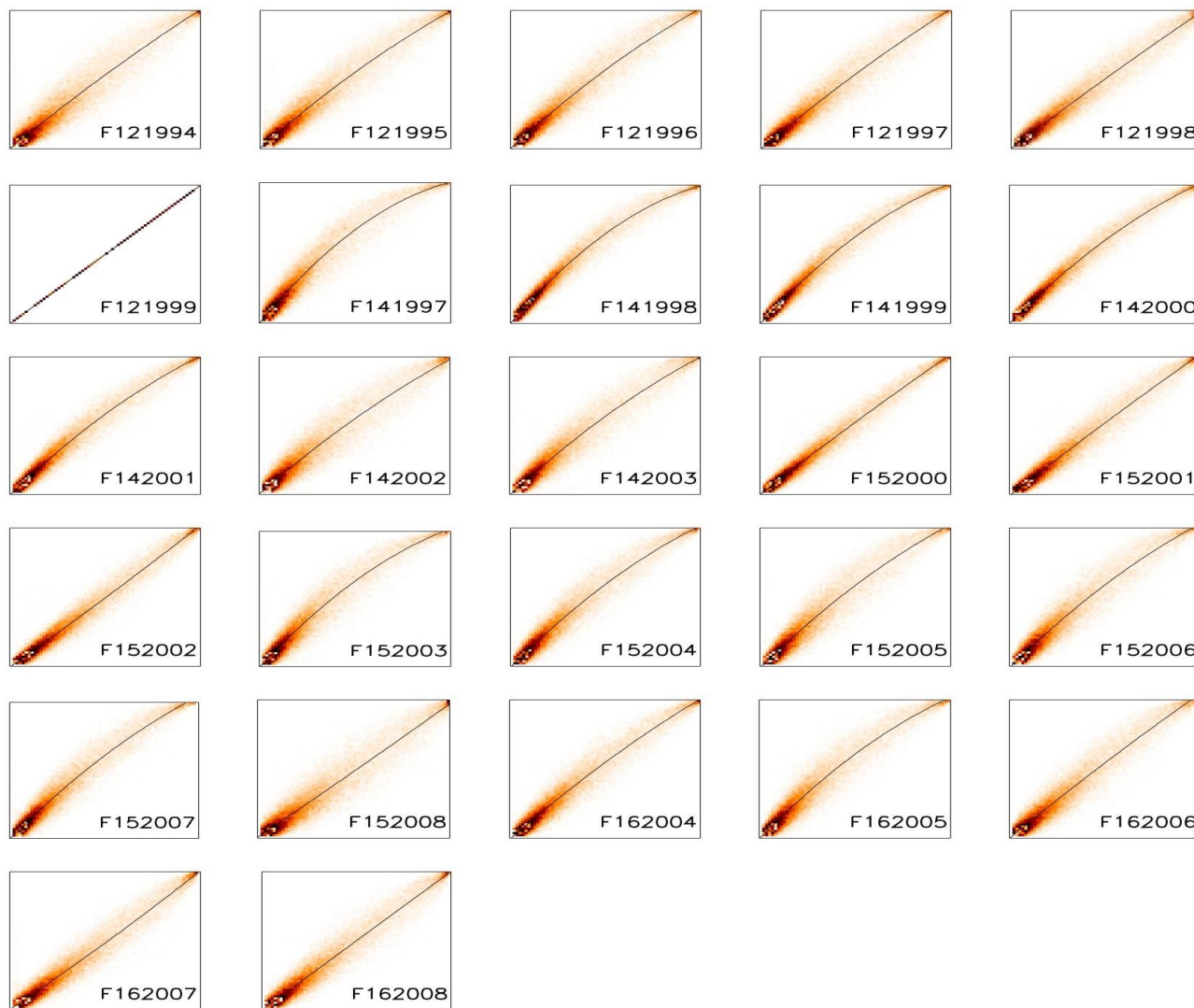
Table 1. Annual composites produced.

Year	Satellite		
1994	F12		
1995	F12		
1996	F12		
1997	F12	F14	
1998	F12	F14	
1999	F12	F14	
2000		F14	F15
2001		F14	F15
2002		F14	F15
2003		F14	F15
2004		F15	F16
2005		F15	F16
2006		F15	F16
2007		F15	F16
2008		F15	F16

2.2. Intercalibration of the Annual Composites

Because the OLS has no on-board calibration the individual composites were intercalibrated via an empirical procedure. Samples of lighting from human settlements (cities and towns) were extracted from numerous candidate calibration areas and examined. In reviewing the data it was found that the data from satellite year F121999 had the highest digital values. Because there is saturation ($DN = 63$) in the bright cores of urban centers and large gas flares, F121999 was used as the reference and the data from all other satellite years were adjusted to match the F121999 data range. In examining the candidate calibration areas it was found that many had a cluster of very high values (including saturated data with $DN = 63$) and a second cluster of very low values. We concluded that having a wide spread of digital number values would be a valuable characteristic since it would permit a more accurate definition of the intercalibration equation. By examining the scattergrams of the digital number values for each year versus F121999 we were able to observe evidence of changes in lighting based on the width of the primary data axis and outliers away from the primary axis. Our interpretation was that areas having very little change in lighting over time would have a clearly defined diagonal axis with minimal width. Of all the areas examined Sicily had the most favorable characteristics – an even spread of data across the full dynamic range and a more sharply defined diagonal clusters of points. Figure 4 shows the scattergrams for each of the satellite years versus F121999 for the nighttime lights of Sicily. The second order regression model was developed for each satellite year is shown in Table 2.

Figure 4. The intercalibration was based on regressions against F121999 images of Sicily (vertical axis). A second order fit is drawn on the density distribution of pixels. Regression results are presented in Table 2.



The objective of the intercalibration is to make it possible to pool the sum of lights index values from each year of the time series. One sign of a successful intercalibration is the convergence of values in years where two satellite products are available. In most cases the intercalibration yielded substantial convergence. Figure 5 shows the raw versus intercalibrated estimates of gas flaring for Algeria. In reviewing the results for many other countries it is clear that the intercalibration brought about substantial convergence. However it was not uncommon for the convergence to be incomplete for one or two years out of the fifteen. An example of this is shown for the 2002 and 2003 Algeria data where the F14 values are lower than those from F15. In reviewing the data from sixty countries there was no obvious pattern in the satellite or year for the cases of incomplete convergence. The lack of full convergence may be caused by diurnal changes in flaring activity since the overpass times of the satellites can differ by as much as two hours.

Table 2. Equations for intercalibrating the annual nighttime lights products. The adjusted digital number (DN) is created by the application of this formula. The coefficients are empirically derived by comparing images of Sicily with F12 1999 (See Figure 4).

$$DN_{adjusted} = C_0 + C_1 \times DN + C_2 \times DN^2$$

SATELLITE	YEAR	C ₀	C ₁	C ₂	R ²	Number
F12	1994	0.1651	1.1244	-0.0018	0.915	38755
F12	1995	0.4103	1.2116	-0.0035	0.937	38795
F12	1996	0.2228	1.2700	-0.0040	0.944	39035
F12	1997	-0.0008	1.1651	-0.0023	0.945	39571
F12	1998	0.1535	1.0451	-0.0009	0.956	39791
F12	1999	0	1	0	1	42780
F14	1997	0.0291	1.6568	-0.0103	0.941	37871
F14	1998	0.1831	1.5980	-0.0096	0.972	37636
F14	1999	-0.1674	1.5116	-0.0078	0.971	38744
F14	2000	0.1061	1.3877	-0.0059	0.972	37769
F14	2001	-0.2595	1.3467	-0.0053	0.963	39389
F14	2002	0.4486	1.1983	-0.0035	0.927	38720
F14	2003	-0.2768	1.2838	-0.0044	0.938	40050
F15	2000	0.1029	1.0845	-0.0010	0.970	39373
F15	2001	-0.4365	1.0850	-0.0009	-0.959	40136
F15	2002	-0.2173	0.9715	0.0008	0.966	40263
F15	2003	-0.2244	1.5238	-0.0079	0.936	38708
F15	2004	-0.3657	1.3772	-0.0056	0.948	39459
F15	2005	-0.6201	1.3504	-0.0049	0.934	39915
F15	2006	-0.6005	1.3551	-0.0049	0.939	39910
F15	2007	-0.1615	1.3960	-0.0054	0.947	38968
F15	2008	0.5031	0.9370	0.0004	0.920	38236
F16	2004	-0.4436	1.2081	-0.0030	0.950	39711
F16	2005	-0.2375	1.4249	-0.0063	0.937	38856
F16	2006	0.0287	1.1338	-0.0013	0.938	38416
F16	2007	0.3210	0.9216	0.0013	0.949	39478
F16	2008	-0.1203	1.0155	-0.0001	0.946	39975

Figure 5. Estimation of gas flaring of Algeria with and without intercalibration of the different satellites.

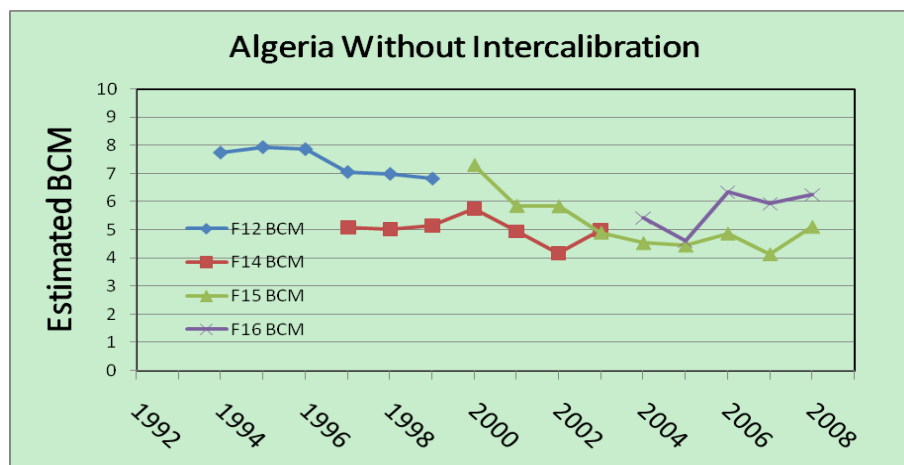
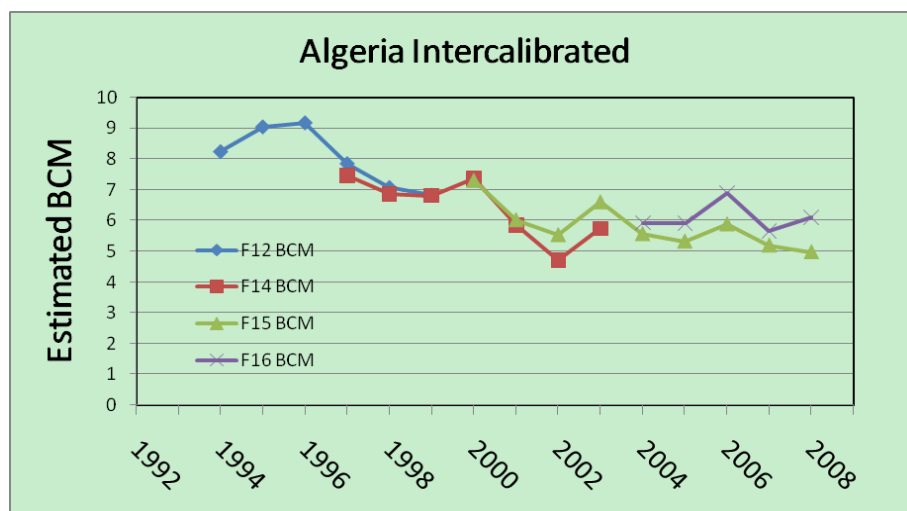


Figure 5. Cont.



2.3. Identifying Gas Flares in DMSP Nighttime Lights

Gas flares are identified visually in the nighttime lights composites. There are three general characteristics for gas flares that provide the visual clues for their identification:

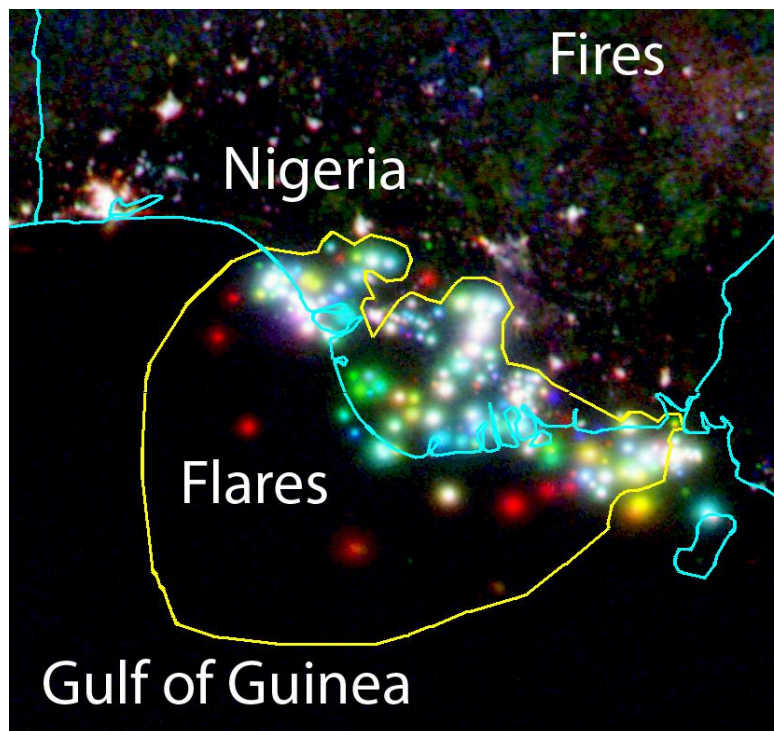
1. Because gas flares are very bright point sources of light with no shielding to the sky, they tend to form circular lighting features with a bright center and wide rims.
2. Most gas flares are active for a period of years, but there are few gas flares that persist with little change in intensity over a full decade. Thus many gas flares exhibit color in blue, green, red images made using data from the beginning, middle and end of the nighttime lights time series. Figure 6 shows an example of this phenomenon for gas flares in Nigeria. The image was made using the nighttime lights from 1994 as blue, 2000 as green, and 2008 as red. Flares active in 2008 but not 2000 or 1994 are red. Those active in 2008 and 2000 are yellow. Those active in 2000 but not 1994 or 2008 are green. Those active in 1994 but not 2000 or 2008 are blue.
3. Gas flares tend to be in remote locations, outside of urban centers. When present offshore they are easy to identify (see Figure 6). For onshore gas flares we reviewed a 30 arc second global population density grid from the U.S. Department of Energy [4] to evaluate lights identified as potential gas flares. In addition, we reviewed NASA MODIS satellite hot spot data, which can assist in clarifying the identity of gas flares on land.

2.4 Confirming the Identity of Gas Flares

Each of the DMSP features suspected to be gas flares was visually inspected in higher resolution remote sensing data available in Google Earth. In many cases it was possible to identify flare stacks, flare pits and even flames associated with the gas flaring (e.g. Figure 7). Approximately 2,500 gas flare features were marked in Google Earth. These placemarks are available at: <http://www.ngdc.noaa.gov/>

dmsp/interest/gas_flares_countries_kmz.html. Features that turned out to be urban or features like airports were marked so that they could be excluded from the set of gas flaring features.

Figure 6. Color composite of the nighttime lights of the Nigeria region generated using 1994 as blue, 2000 as green, and 2008 as red. The colors of the flares indicate their activity patterns during the three years used in the color composite. Note the six red offshore flares, indicating the increase in offshore oil production in 2008 relative to 2000 and 1994. The vector polygon drawn around the gas flares of Nigeria is shown in yellow. The diffuse light in the upper right is from biomass burning.



2.5. Vectors and Extractions

Using these three visual criteria and the Google Earth inspection it is possible to manually draw vector polygons to identify the gas flares for individual countries. Figure 6 shows an example of the vectors drawn for the country of Nigeria. An extraction was then run on the sum of lights and cloud-free coverage Mollweide projection images. The extracted fields include the area of lighting detected, the number of saturated grid cells, the minimum, maximum and average number of cloud-free observations encountered under the polygon vectors, and the sum of lights index. The extraction produces a text file (csv) that can be imported into a spreadsheet for analysis and plotting.

Figure 7. The identification of three flames at a gas flaring location using the high resolution base imagery available in Google Earth. Each of the DMSP identified gas flare locations were inspected in Google Earth for visual confirmation of the feature and to eliminate the inclusion of human settlements and features such as airports from the final set of gas flare features. A total of 2,500 gas flaring features were identified using Google Earth.



2.6. Calibration to Estimate Gas Flaring Volumes

A calibration was developed to estimate gas flaring volumes for individual countries based on the sum of lights index values and a set of reported gas flaring volumes for countries and individual flares (Figure 8). The steps in developing the calibration include:

1. Gathering reported flaring volumes.
2. Associating them with observed flares.
3. Determining the calibration coefficient that relates the observed sum of lights index to the flaring volume.
4. Establishing the prediction interval of the calibration coefficient.

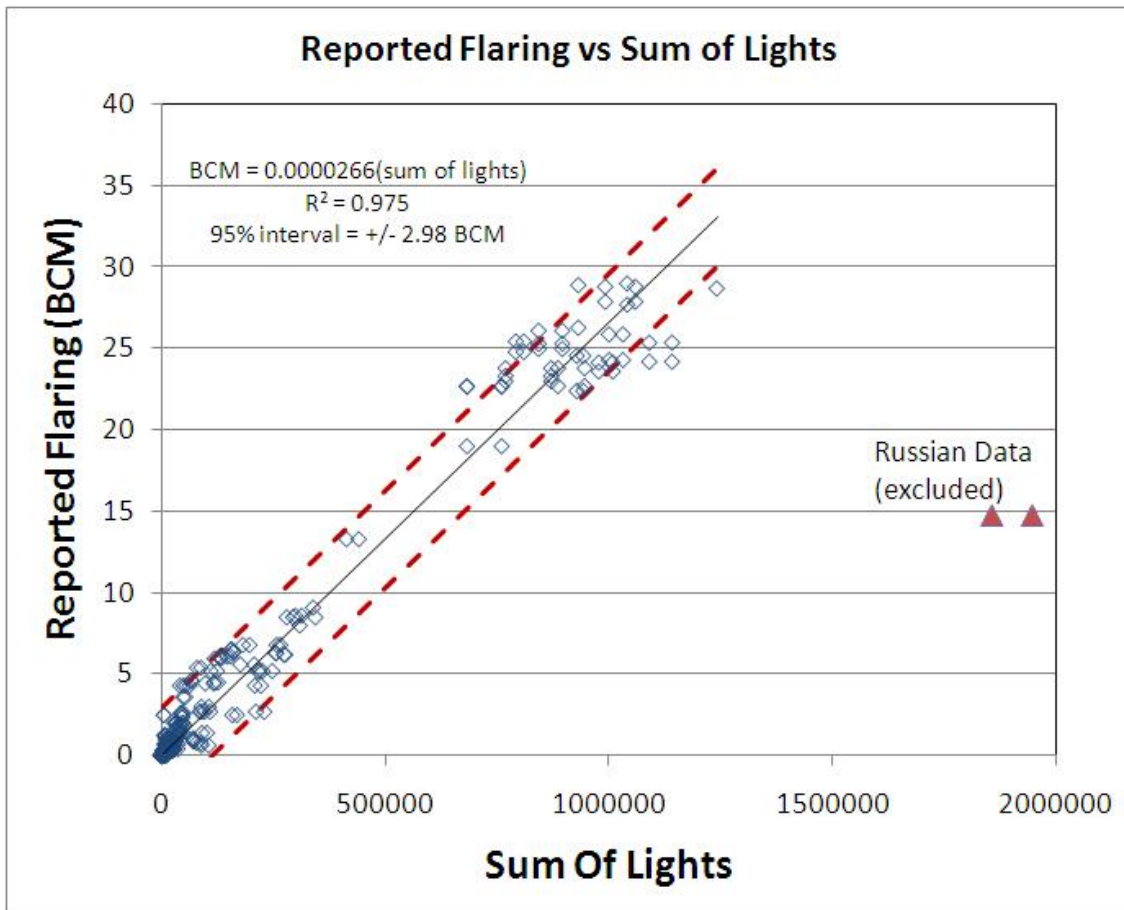
Gathering reported flaring volumes: All of the reported BCM values available from the GGFR Partnership were considered. This includes the reported country-wide data GGFR has gathered from 2004 onward, as well as from a number of individual flares (or flare sets). The Russia data were discarded *a priori* based on visual examination of the scattergram of the sum of lights index versus BCM (see Figure 8).

Associating flares with reported BCM: Each flare for which we had reported data was visually inspected on the DMSP images and with Google Earth. If flares were packed too tightly to isolate from their neighbors then the entire cluster was grouped together and the reported flaring volume for the flares in that cluster was aggregated. A map of the Exclusive Economic Zone (EEZ) for each country was overlaid on the flares to ensure that offshore flares were correctly attributed to their national hosts.

Determination of the Calibration Coefficient: A linear regression model was used with a zero intercept. The model is: $BCM = 0.0000266 \times \text{Sum of lights index}$, $R^2 = 0.976$.

Establishing the prediction interval: After obtaining the least squares estimation equation, we used it to make predictions of the BCM of flared gas for the calibration data. The predicted flaring volume is subtracted from the reported amount. The absolute value of this difference is the residual. The “prediction interval” is determined when 95% of the residuals are smaller than that value. The prediction interval was found to be 2.98 BCM. In other words, 95% of the residuals of the calibration data were smaller than 2.98 BCM. This prediction interval is carried through the analysis as the error associated with our gas flaring estimates.

Figure 8. Plot of the reported BCM levels of flared gas versus the sum of light index, regression line (solid line) and 95% prediction intervals for individual BCM estimates (dashed red lines).



3. Results and Discussion

3.1. National Gas Flaring Estimates for 2008

Gas flaring volumes were estimated for individual countries based on the sum of lights index values. The estimates for the top 20 individual countries for the year 2008 are shown as a bar chart in Figure 9 and listed in Table 3. The estimates indicate that the quantity of gas flaring is concentrated in a small number of countries. Russia had the largest gas flaring volume, with 40 BCM in 2008, followed by Nigeria at 15 BCM. Together Russian and Nigeria account for 40% of global gas flaring and the top twenty countries account for 85%.

Figure 9. Year 2008 gas flaring estimates in billions of cubic meters (BCM) for the top 20 countries.

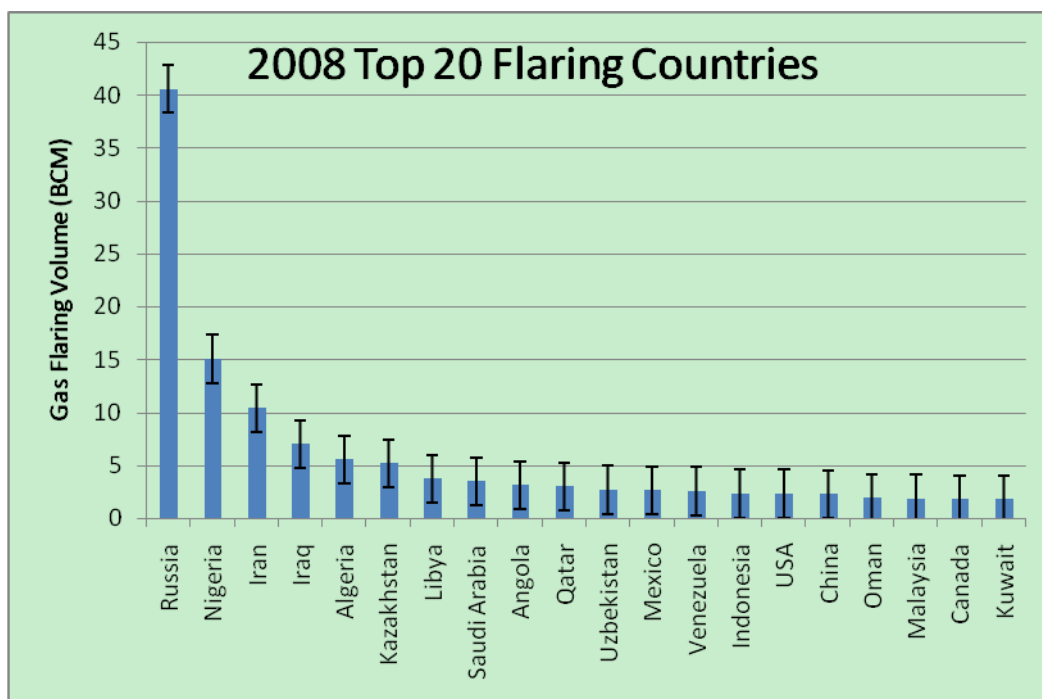


Table 3. Year 2008 top twenty gas flaring countries.

Rank	Country	Gas Flaring (BCM)	Estimated Error (+/- BCM)
1	Russia	40.5	2.11
2	Nigeria	15.1	2.11
3	Iran	10.4	2.11
4	Iraq	7.0	2.11
5	Algeria	5.5	2.11
6	Kazakhstan	5.2	2.11
7	Libya	3.8	2.11
8	Saudi Arabia	3.5	2.11
9	Angola	3.1	2.11
10	Qatar	3.0	2.11
11	Uzbekistan	2.7	2.11

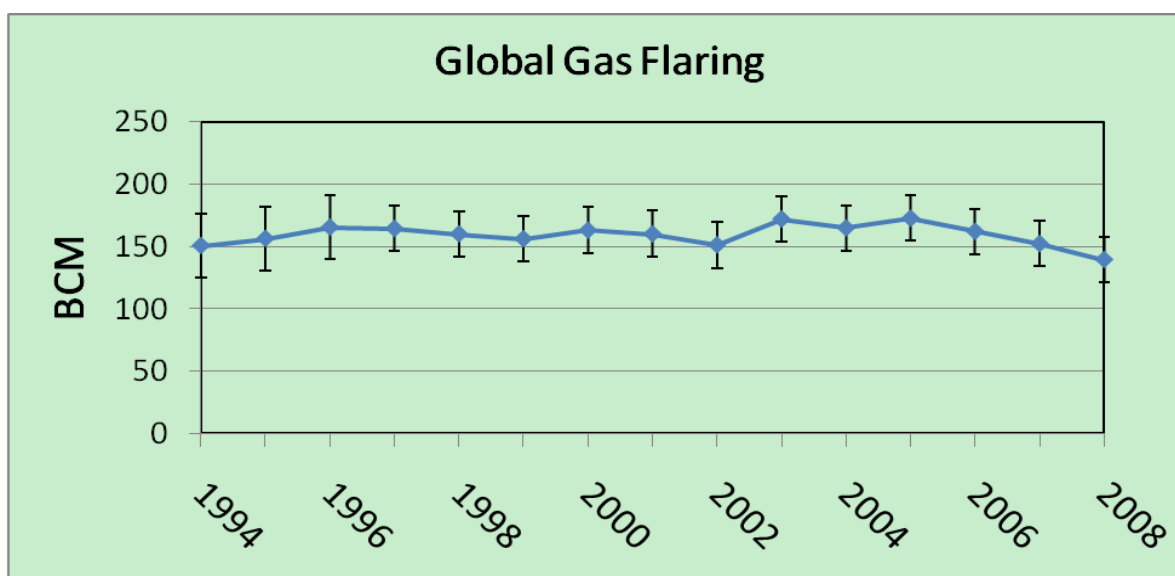
Table 3. Cont.

12	Mexico	2.6	2.11
13	Venezuela	2.6	2.11
14	Indonesia	2.3	2.11
15	USA	2.3	2.11
16	China	2.3	2.11
17	Oman	1.9	2.11
18	Malaysia	1.9	2.11
19	Canada	1.8	2.11
20	Kuwait	1.8	2.11

3.2. Trends over Time

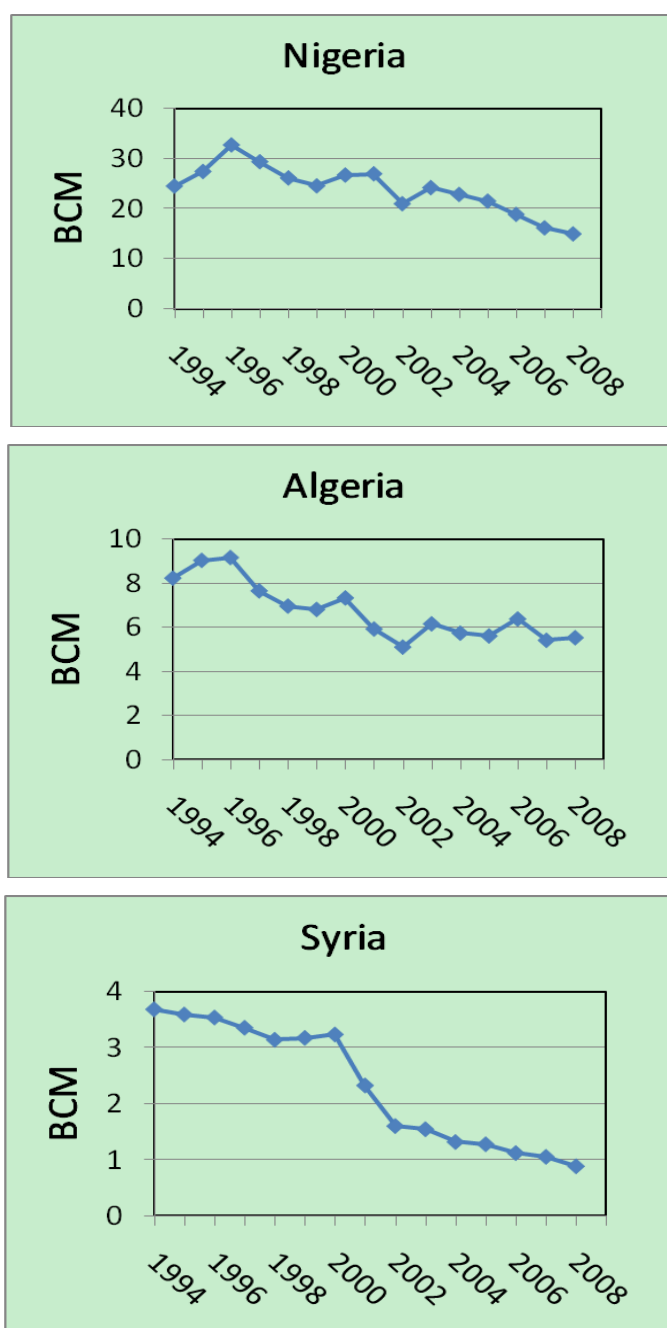
With a fifteen year record of gas flaring it is possible to observe patterns or trends in gas flaring activity over time. The DMSP estimates of flaring have remained largely stable between 140 and 170 BCM from 1994 to 2008 (Figure 10). The estimates show a slight peak in 2005 and have been declining steadily since then. The DMSP data indicate global gas flaring has decreased by 19% since 2005, from 172 to 139 BCM. In analyzing the national trends we divided the temporal record into two segments divided at the year 2005 peak in global flaring. In the early segment (1994 to 2005) we defined four broad categories: decreasing, peak-in-the-middle, stable, and increasing.

Figure 10. Global gas flaring volume has been in the range of 140 to 170 BCM from 1994 to 2008. The peak was 2005 with 172 BCM and flare volume has been declining since that time. The estimated error (σ) of each global total is generated from the square root of the sum of errors of each country squared (σ_i^2). In years where estimates were made using data from a single satellite the estimated error is 23.8 BCM (1994, 1995, 1996). In subsequent years the estimated error is reduced to 16.9 BCM based on the inclusion of separate flare volume estimates from two satellites.



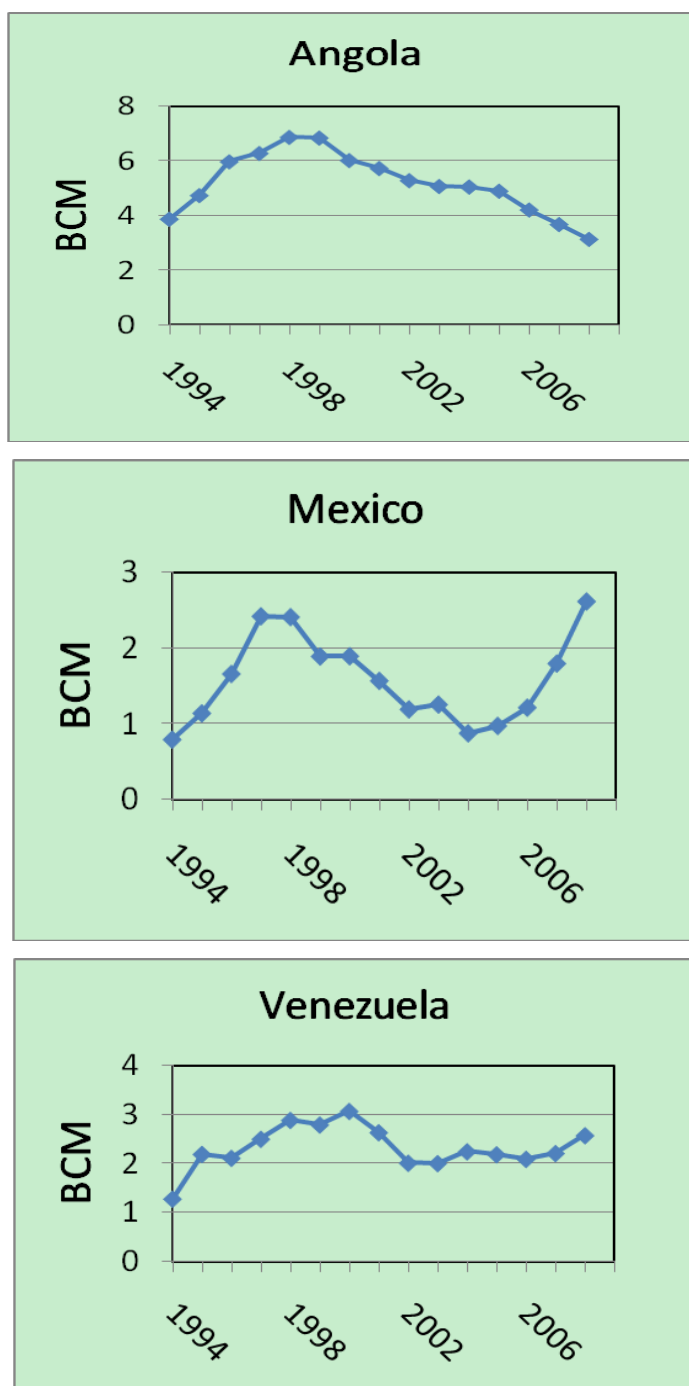
Decreasing: Seventeen countries exhibited a downward trend in estimated gas flaring from 1994 to 2005, including Algeria, Argentina, Bolivia, Chile, Egypt, India, Indonesia, Libya, Netherlands, Nigeria, Norway, Peru, Syria, UAE, UK and USA. The results for Nigeria, Algeria and Syria are shown in Figure 11. Nigerian gas flaring has had several ups and downs – but the overall reduction in gas flaring is in the range of 10 BCM. Algeria and Syria had decreases better than 2 BCM since 1994.

Figure 11. Nigeria, Algeria and Syria were three of the seventeen countries where gas flaring declined over the 1994 to 2005 time period. For Nigeria and Syria the decline continued from 2005 to 2008. Algeria’s gas flaring was largely stable in recent years. Note that the estimated error in the data presented in Figure 11 to 14 is 2.98 BCM for 1994 through 1996 (one satellite) and 2.11 BCM for 1997 through 2008 (two satellites).



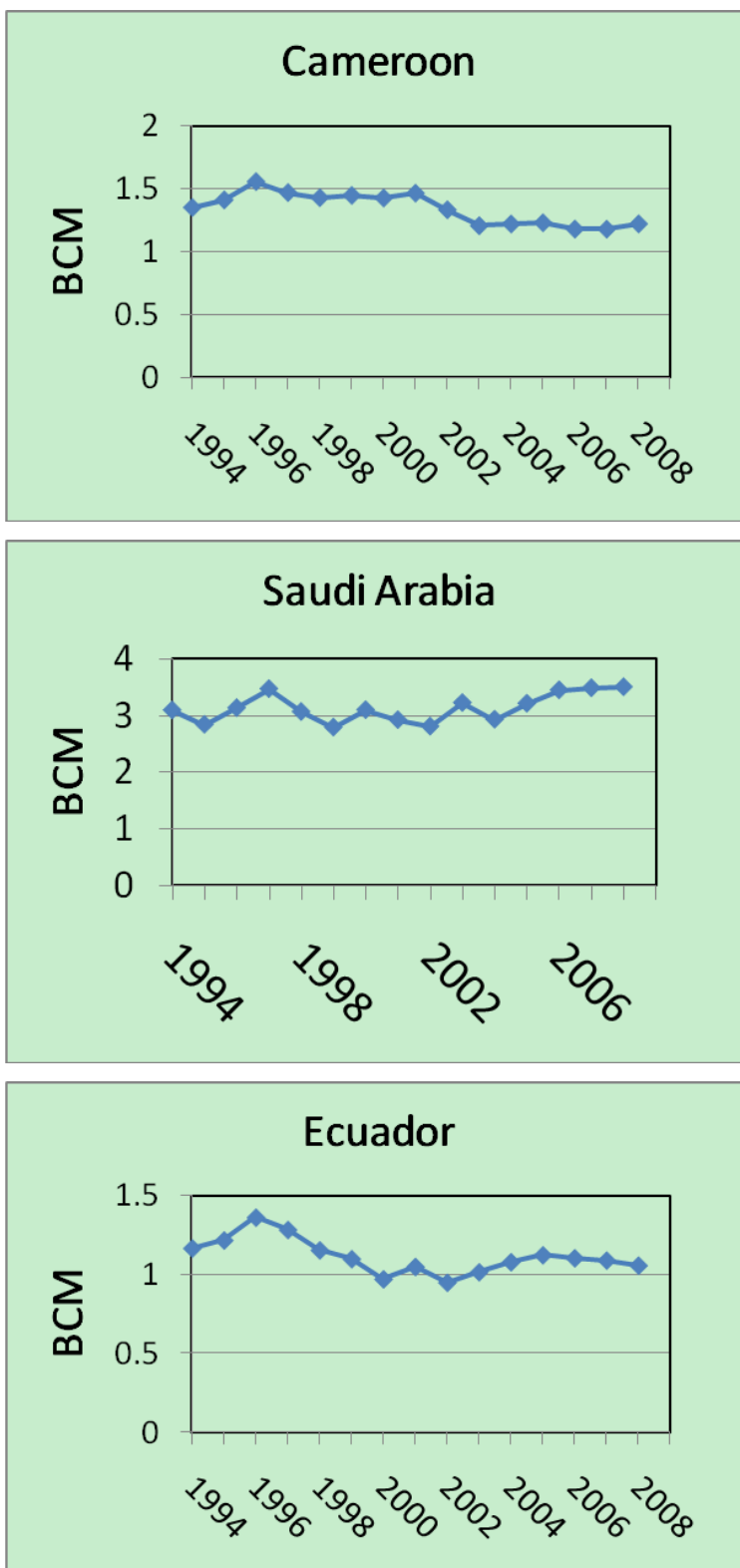
Peak-In-The-Middle: Seventeen countries had peaks in estimated gas flaring between the end points of the time series (1994 to 2005) – but nearly the same quantity of gas flaring in recent years as in the mid-1990’s. This includes Angola, Brazil, Brunei, Canada, Colombia, Congo, Cote d’ Ivoire, Democratic Republic of Congo, Denmark, East Timor, Mexico, Papua New Guinea, Philippines, Trinidad, Venezuela and Vietnam. Figure 12 shows three examples of this pattern.

Figure 12. Angola, Mexico and Venezuela were three of the seventeen countries that exhibited a gas flaring peak near the middle of the time series. Gas flaring in Angola has been steadily declining in recent years. In contrast Mexico had a major increase in gas flaring from 2005 through 2008.



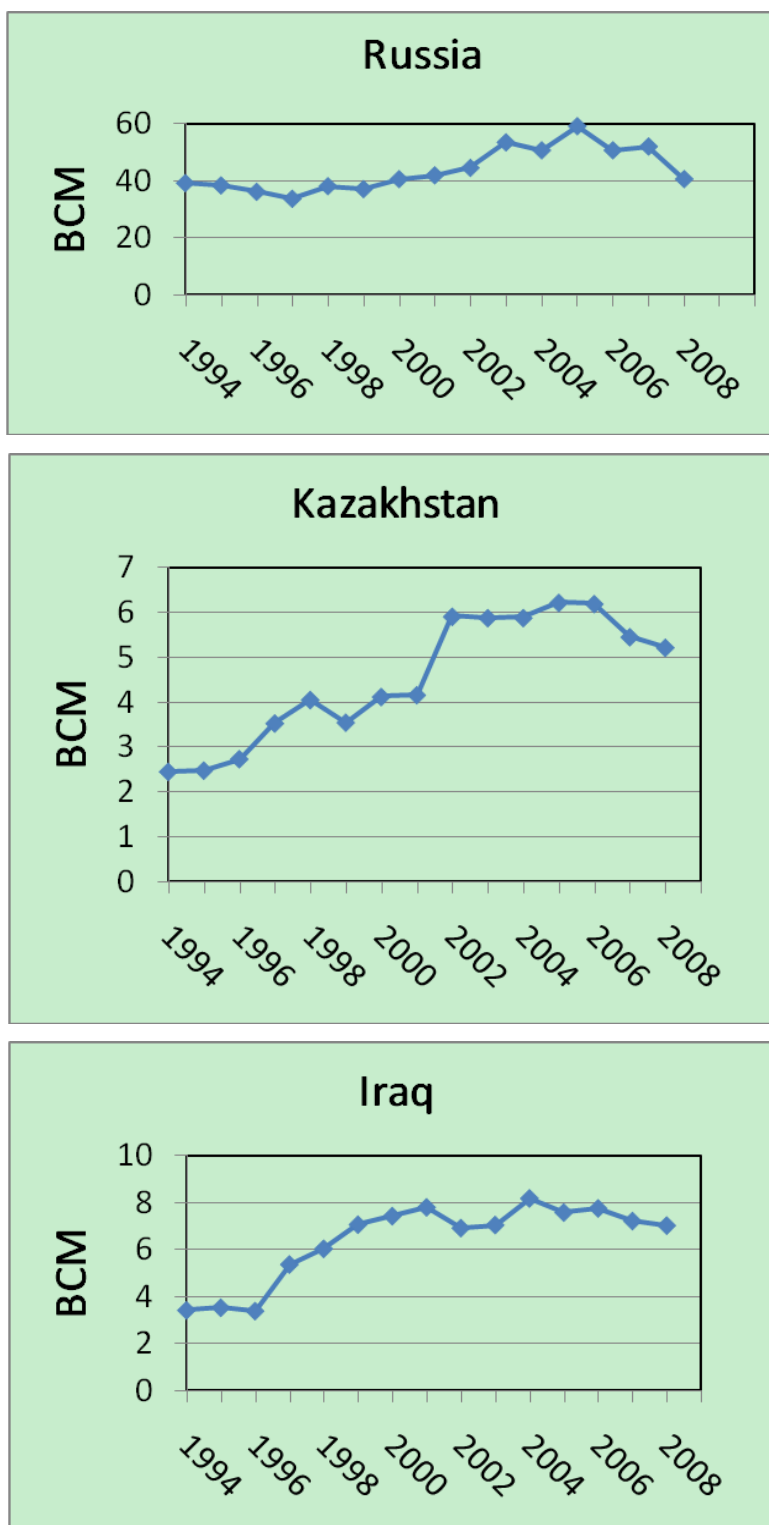
Steady Flaring: Nine countries had largely stable estimated gas flaring across the time series. In some cases there were ups and downs – but no obvious trend. This includes Cameroon, Ecuador, Gabon, Iran, Kuwait, New Zealand, Romania, and Tunisia. Figure 13 shows the results for Cameroon, Saudi Arabia and Ecuador.

Figure 13. Cameroon, Saudi Arabia, and Ecuador were three of the nine countries or areas where gas flaring volumes remained largely stable over the years examined.



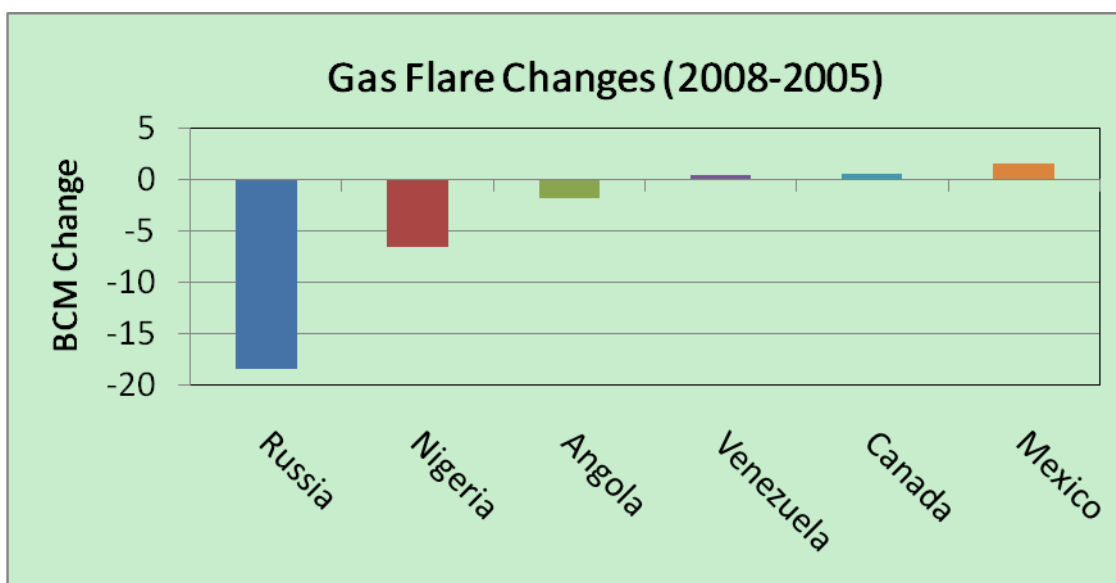
Increasing: Seventeen countries have an upward trend in gas flaring over the 1994–2005 range. This includes Azerbaijan, Chad, China, Equatorial Guinea, Ghana, Iraq, Kazakhstan, Myanmar, Oman, Qatar, Russia, South Africa, Sudan, Thailand, Turkmenistan, Uzbekistan, and Yemen. Figure 14 shows the results for Russia (with a gain of 20 BCM), Iraq (+4 BCM) and Kazakhstan (+3 BCM).

Figure 14. Russia, Kazakhstan and Iraq were three of the seventeen countries where gas flaring volumes increased from 1994 to 2005. Gas flaring declined in all three countries from 2005 through 2008.



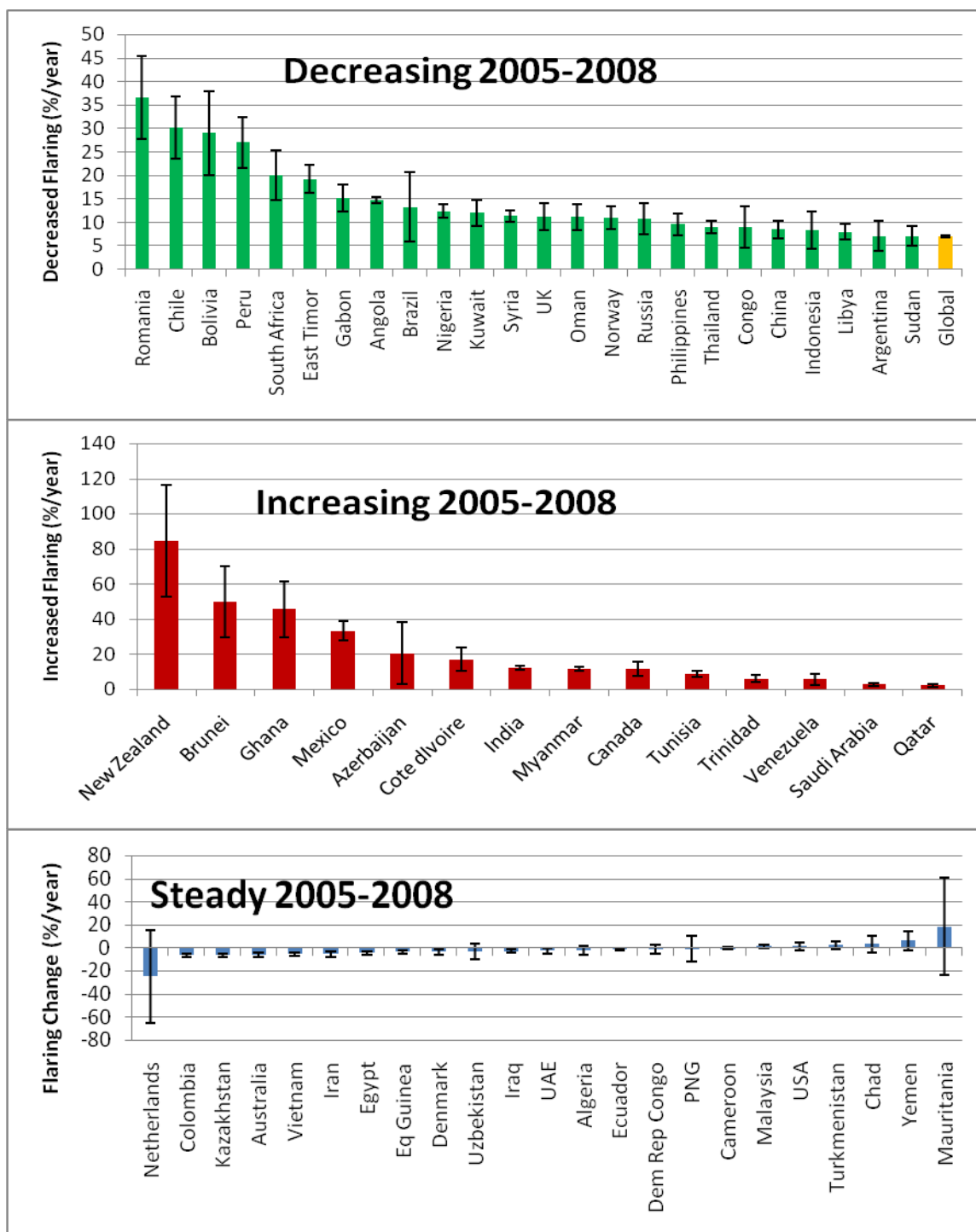
The global BCM results indicate that a decline in gas flaring activity has occurred in each year following the peak in 2005. We have analyzed the BCM estimates from the individual countries to identify the source of the declines. In comparing the top three countries with declining gas flaring with the top three countries with increases (Figure 15) it can be seen that Russia and Nigeria lead the decline with 18.5 and 6.5 BCM declines respectively, followed by Angola with a 1.8 BCM decline. Russia and Nigeria account for 75% of the total decline in gas flaring from 2005 to 2008. Of the eight countries with increased flaring Mexico led with an increase of 1.6 BCM from 2005. The total BCM gain from all the increasers is 2.6 BCM, equivalent to 10% of decrease observed for Russia, Nigeria, and Angola combined.

Figure 15. Comparison of the change in flaring from 2005 to 2008 for the top three countries showing decline (Russia, Nigeria and Angola) versus the three countries with the most increase in flaring over the same time period (Venezuela, Canada, and Mexico). Russia led in flaring reduction with a decline of 18 BCM. The total decline for Russia, Nigeria and Angola (−26 BCM) was ten times more than the increase in flaring for Venezuela, Canada and Mexico (2.6 BCM).



The rate of change over the last four years (2005–2008) was computed by converting each country’s flaring to a percent change relative to the 4-year mean for that country. Then a best-fit regression was calculated and a 1-sigma uncertainty for that slope. If the slope was negative and its absolute value was larger than its uncertainty, we classified that country as “Decreasing” (see Figure 16). Likewise, if the slope was positive and larger than its uncertainty, the country was classified as “Increasing”. If the absolute value of the slope was smaller than the uncertainty, then the country was classified as “Steady”. A “Steady” classification is ambiguous since it could be either a situation of little change or erratic change that makes the identification of the trend highly uncertain. Since 2005, the estimated global gas flaring has declined by 33 BCM. The trend from 2005 to 2008 shows thirty-three countries with declining gas flaring, fifteen countries with stable gas flaring, and only eight countries with increasing gas flaring.

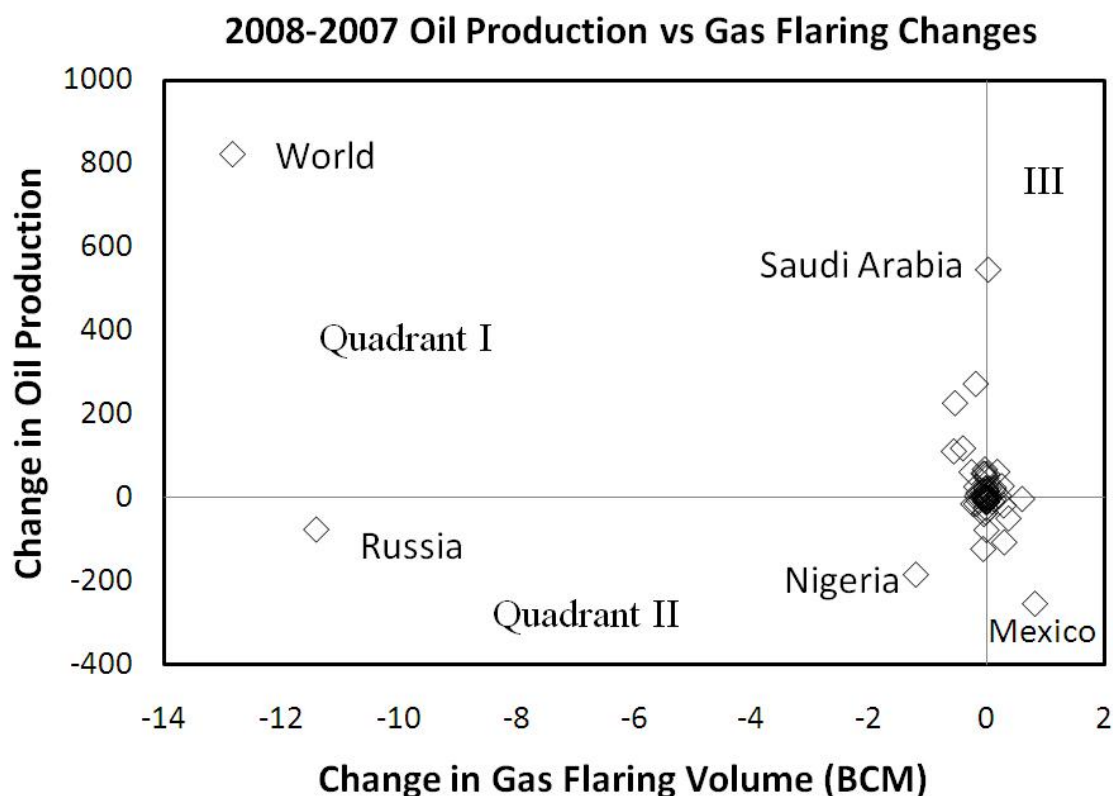
Figure 16. Flaring trends over the last four years (2005–2008). The rate of change over the years is plotted for each country where gas flaring was detected. They are grouped as “Decreasing” if the rate of change is negative (and less than the uncertainty in the determination of the slope), “Increasing” if the rate is positive, and “Steady” if the absolute value of the slope is smaller than its uncertainty. Note that some countries with small decreases in gas flaring activity countries are rated as “steady” based on the uncertainty of the change. The error bars indicate the uncertainty in the rate of change.



3.3. Efficiency

Another approach for analyzing recent changes in flaring activity is to compare changes in flare volume estimates to changes in oil production reported by the U.S. Department of Energy, Energy Information Administration [5]. Figure 17 plots the change in flaring volume with change in oil production (2008 minus 2007). Surprisingly, increased production does not seem particularly correlated with increased flaring. Rather, there is a weak trend correlating increasing production with a decrease in flaring ($R^2 = 0.23$). The global total which shows an overall increase in production and decrease in flaring is dominated by a few countries. Russia and Nigeria combined account for 98% of the global decrease in flaring. Saudi Arabia and Iraq combined account for 99% of the increased production in 2008.

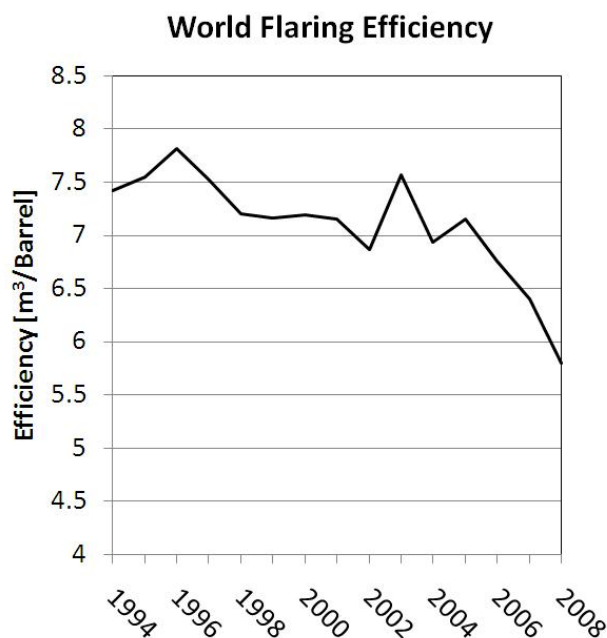
Figure 17. Changes in national and global flaring versus change in oil production from 2007 to 2008. In Quadrant I crude oil production increased while gas flaring declined. This includes the global total (World) plus the countries Angola, Iran, Iraq, and Kuwait. Saudi Arabia expanded their production by 7.5% while their flaring volume remained essentially unchanged. Quadrant II countries had reduced crude oil production and decreased gas flaring (Nigeria and Russia). Quadrant III countries had increased crude oil production and increased gas flaring. Quadrant IV countries had reduced crude oil production with an increase in gas flaring (Mexico, USA, Uzbekistan, and Venezuela).



The fact that both gas flaring and crude oil production declined from 2007 to 2008 for Russia and Nigeria raises the question—is the gas flaring decline due to dropping oil production? It is known that

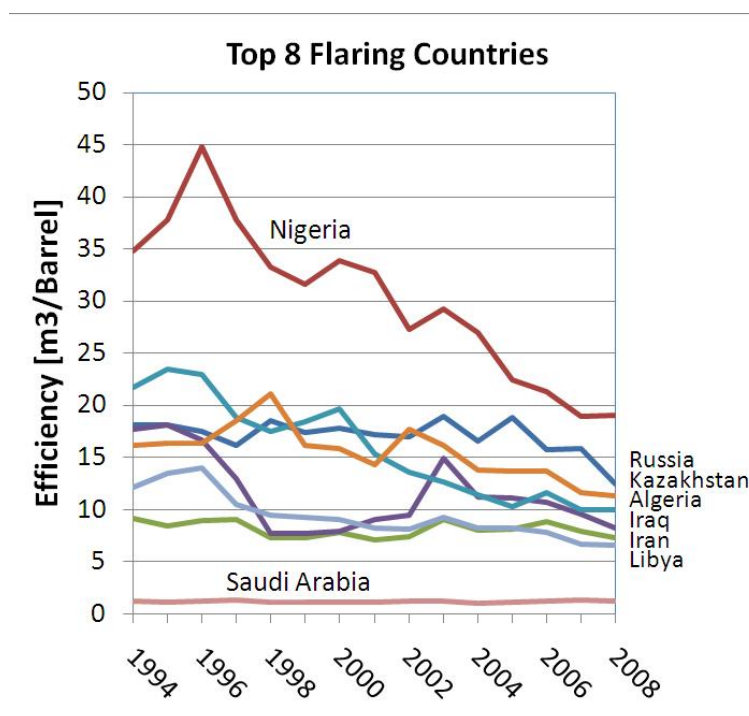
oil production in Nigeria has frequently been disrupted in recent years by civil unrest and sabotage. To investigate the influence of oil production changes on gas flaring volumes we calculated gas flaring efficiency as the volume of gas flared per barrel of crude oil produced. In 2008, 139.37 BCM was flared and the world crude oil production [5] was 65848.3 kB/day (Thousand Barrels of Crude Oil per day). This number (and all other quotes of Crude Oil production) was derived as the Crude Oil (including Natural Gas Plant Liquids and Other Liquids) minus the Natural Gas Plant Liquids. If we take the ratio on an annual basis for 2008, the global efficiency is 5.6 m^3 gas flared per Barrel of Oil. Comparing the energy content of gas to crude oil, this represents a waste of 3.5%. When this calculation is extended over the available time series (Figure 18) the results indicate that flaring efficiency has improved steadily from 2005 through 2008. In fact, 2007 and 2008 were the most efficient years over the entire fifteen year period.

Figure 18. Global gas flaring efficiency ranged from seven to eight cubic meters per barrel of oil from 1994 to 2005. Since 2005 the efficiency has improved for three years in a row and stood at 5.6 m^3 per barrel in 2008.



We examined the flaring efficiencies for individual countries and found that there is substantial variation among the countries and trends in efficiency over time for individual countries. Figure 19 plots the annual flaring efficiencies for the top eight flaring countries. Nigeria has the worst efficiency of this group, but exhibits a trend for improved efficiency since 1996. Similarly Algeria exhibits a trend for improved flaring efficiency since the mid-1990s. Iraq had its best flaring efficiency from 1998 through 2002, but has been improving its flaring efficiency since 2003. Kazakhstan has been improving its flaring efficiency since 2002 and Russia has been improving since 2005. Saudi Arabia is one of the most efficient oil producers in the world in terms of gas flaring. Because the gas flaring efficiency has improved in both Russia and Nigeria from 2005 through 2008 we conclude that the observed reduction in gas flaring volume cannot be solely attributed to declines in oil production.

Figure 19. Gas flaring efficiency of the top eight flaring countries. Efficiency is defined as the volume of gas flared per barrel of crude oil produced. Nigeria is least efficient, but seems to be improving with time. Saudi Arabia consistently out performs the other top flaring countries implying that it is quite efficient in the utilization of associated gas.



There are several factors which may affect the efficiency results in addition to changes in gas utilization practices. If more gas is vented (without flaring) or re-injected into the ground the satellite data would likely find that there had been an increase in flaring efficiency. There is variation in the gas content of crude oil from different fields and gas-to-oil ratios can change gradually over time. Changes in the gas-to-oil ratio are sufficiently gradual that this could only be a minor component in the trend observed from 2005 to 2008, where global gas flaring declined by 19%. A change in the diurnal or seasonal pattern of flaring could also affect the efficiency calculation since the DMSP sensor only detects flaring in the early evening and data from mid-to-high latitudes are not usable in mid-summer due to solar contamination of the nighttime visible band data. Certainly under or over reported oil production would have a direct effect on the calculated efficiency, as well as errors in our identification of flares. Among the countries which improve their flaring efficiency we are not able to determine whether this indicates a change in the gas content of the oil, improved capture and utilization of the associated gas, an increase in reinjection, or more venting of unburned gas.

3.4. Sources of Error and Uncertainty

There are a number of sources of uncertainty and error in the results of this study. To the extent to which these errors are present in the calibration data (see Figure 8) these sources of uncertainty contribute to the ± 2.98 BCM prediction interval. The sources of error or uncertainty include:

Errors in the reported flare volume data: There are surely errors in the reported gas flaring data used in the calibration shown in Figure 8. Flaring data reported by different sources often differ with no clear way to determine the “best” value. In addition to these general uncertainties, there are also a number of known uncertainties in the reported data.

For Russia, the reported volumes only include flared volumes of gas associated with oil production. In addition to this flaring, there is known to be a very significant volume of gas flared from condensate stripping ventures. This likely contributes to the satellite data finding that Russia gas flaring is substantially higher than previously reported.

For many countries (including USA, Venezuela, Brazil and Indonesia) the reported flare volumes include unknown quantities of vented gas in addition to the flared gas. Since the DMSP only detects flared gas, if there is significant vented gas the satellite estimates will be lower than the reported values. In addition, flares combust less than 100% of the gas going to the flare stack. The reported data, including that used in the satellite calibration, is the gas volume going to the flare stack while the satellite can only detect the portion being burnt. While the calibration procedure will adequately correct for the ‘average’ flare inefficiency, differences in the efficiency of individual flares will introduce scatter in the data.

Variations in flare quality: The volume of gas present in the oil, the procedures used in oil/gas separation, and the type of equipment used for the flaring all affect the quality of the flaring and the amount of light emitted for detection by the satellites. For instance it is possible that a smoky flare will have more of the light absorbed by soot particles, which may reduce the brightness of the flare.

Mis-identification of flares: The careful inspection of possible flares with Google Earth has greatly diminished the mis-identification of flares. We have continuously improved our ability to distinguish flares from other lights. However, we have generally restricted our measurements of flares to those that are isolated from incidental lighting such as urban areas and industrial complexes. We acknowledge that the identification of flares requires some subjective judgment and small errors associated with both omissions and inclusion of non-flare related light occurs.

Non-continuous sampling: It is possible for flaring activity to vary substantially over the course of a year or even within a single day. The data used in this analysis are all from the early evening (7 to 10 p.m.) and have been screened for factors such as sunlight, moonlight and clouds to produce a uniform product from year to year. The screening to exclude sunlit data combined with an early evening overpass time results in an absence of samples during summer months at high latitudes. In total most flares have 40 to 80 valid samples in a year (see Figure 2). Since the OLS sensors acquire six scan lines per second—the cumulative observation time for 60 valid samples is only 10 seconds! In some cases the temporal distribution of the valid observations may not have been sufficient to capture a representative sum of lights index. Due to the launch dates and sensor or orbit degradations it was not possible to include a full year of observations in each of the satellite products. The most conspicuous example is the F121994 product, which only includes data from the last four months of 1994 since it began collecting data in September.

Environmental effects: There are some environmental conditions which contribute to either reductions or enhancements to the quantity of light from gas flares that escapes into space for detection by the OLS. Countries like Saudi Arabia and Algeria have very dry atmospheres with slightly less attenuation of light into space as compared to the humid tropical atmospheres present in countries such as Nigeria and Indonesia. One environmental effect that has been studied, but is not yet corrected for is the difference in surface reflectance between onshore and offshore flares. Because the flares are unshielded they emit light in all directions. For that portion of the light that is emitted in a downward direction (towards the ground) there is a possibility that the photons will either be absorbed by the surface or reflected. It was observed that offshore flares are slightly dimmer for a given gas flare volume than their onshore counterparts. We are investigating options for the correction of this bias. A similar investigation on the effects of snow cover found that the sum of lights index was not affected by the presence of snow cover.

Persistent lighting at petroleum facilities: Outdoor lighting present at the flare facilities has been included in the sum of lights index values. This increases the sum of lights index values. To the extent that all flaring sites have outdoor lighting present—the added brightness is present in all the calibration data and does not adversely impact the calibration. Variations in the outdoor lighting present at the flaring sites has undoubtedly contributed to the prediction interval (or error bars) shown in Figure 8.

OLS sensor differences: It is known that the optical throughput of orbiting sensors tends to decline over time due to the accumulation of dust on mirrors. Detectors, stabilizing gyroscopes and electronics can all degrade over time and effect data quality. The intercalibration procedure was designed to account for as many of these effects as possible. But the intercalibration procedure may not have fully addressed differences in the spectral bandpasses of the different OLS sensors. The reference data used in the intercalibration were electric lights not gas flares. The OLS nighttime “visible” band straddles the visible and near infrared portion of the spectrum. Based on Wein’s Law gas flares are expected to have higher radiant emissions in the near-infrared than in the visible portion of the spectrum. Thus variation in the throughput of the near infrared portion of the OLS sensor bandpasses might impact the comparability of results from different satellites.

4. Conclusions

The first globally consistent survey of gas flaring has been conducted using satellite data. The survey spans a fifteen year period from 1994 through 2008. Global gas flaring has remained largely stable over the past fifteen years, remaining in the range of 150 to 170 BCM. The global gas flaring estimate for the year 2008 is 139 BCM, a little over 4% of the global natural gas production. This gas flaring represents an added carbon dioxide equivalent emission burden to the atmosphere of about 278 million metric tons—equivalent to the annual carbon emissions from 50 million passenger cars in the USA. If the 139 BCM of flared gas were sold in the USA at 2008 prices—the retail value would have been \$68 billion based on pricing data from the U.S. Department of Energy. Gas flaring estimates were produced for sixty countries. While Nigeria has been widely reported as the country with the largest volume of gas flaring, this is not supported by the satellite data, which indicate that Russia has more

than twice the gas flaring volume of Nigeria. The satellite data indicate a 19% reduction in gas flaring volumes from 2005 to 2008, led by gas flaring reductions in Russia and Nigeria. There are six possible mechanisms for the observed gas flaring reductions: (1) increased utilization, (2) decreased oil production, (3) increased reinjection of gas, (4) increased venting, (5) reduction in the gas-to-oil ratios, and (6) reducing flare activity at the time of the satellite overpasses. Both Russia and Nigeria have made efforts to move associated gas to markets. However, the natural gas volumes associated with these projects are unknown. Crude oil production has declined in recent years in both Russia and Nigeria, which accounts for a portion of the decline. However, both countries improved their gas flaring efficiencies from 2005 through 2008, indicating that the decline in gas flaring cannot be fully explained by reduced crude oil production. There are no reported data on reinjection or venting volumes, so it is possible that a portion of the decline in gas flaring observed in Russia and Nigeria are due to changes in these practices. Gas-to-oil ratios are known to change slowly within individual production reservoirs as they mature. In both Russia and Nigeria the DMSP data show some flares going out and new flares being established in other locations on an annual basis. This turnover in the spatial location of active flares suggests the tapping of new reservoirs for crude oil production. Given the large number of flares active in both countries and the turnover which is occurring, changes in the gas-to-oil ratio could only be playing a minor role in the gas flaring volume changes observed from 2005 through 2008. The possibility that diurnal pattern of flaring activity might have been reduced during the early evening hours when the DMSP satellites collect data, either intentionally or unintentionally, cannot be discounted. While the satellite results are consistent with improved capture and utilization of associated gas, we have insufficient information to draw any conclusions on how the gas flaring reductions were achieved in Russia and Nigeria.

The DMSP-OLS archive has provided a fifteen year record of global gas flaring. However, if one were to design a satellite sensor specific to the global monitoring of gas flares it would be substantially different from the DMSP-OLS. While gas flares are readily identified offshore in OLS data, it was not possible to identify gas flares imbedded in the lighting present in urban centers. Identified shortcomings of the OLS [6] include: (1) coarse spatial resolution, (2) lack of on-board calibration, (3) lack of systematic recording of in-flight gain changes, (4) limited dynamic range, (5) six-bit quantization, (6) signal saturation in the cores of many gas flare features, (7) lack of specific spectral bands tailored for measuring flare size, temperature gaseous composition and combustion efficiency. Improvements in some of these areas are anticipated with the launch of the Visible Infrared Imaging Radiometer Suite (VIIRS) in the 2012–2020 time range. There are also a number of current sensors, such as NASA's Moderate Resolution Imaging Radiometer System (MODIS) and the Indian Resourcesat AWiFS sensor that have potentially high value in global monitoring of gas flares that have yet to be fully explored. We fully expect that improvements in the estimation of gas flaring volumes will be achieved in the future through the inclusion of multiple satellite data sources. It is also clear that improvements in satellite estimates of gas flaring will require reliable sources of reported and metered gas flaring volumes for calibration. The following is a list of possible next steps aimed at improving the accuracy of the gas flaring estimates and understanding the effectiveness of flaring reduction efforts.

Improved intercalibration: We are working on a second approach to intercalibration that makes no reliance on the assumption that lighting for a reference area has been largely stable over time. The alternate approach is based on tracking the brightness of desert surfaces under full moon conditions. If successful, this may reduce the uncertainties associated with the current intercalibration which assume that the lighting in Sicily has been largely stable.

Integration of additional high temporal resolution imagery: Fire detection data from systems such as NASA's Moderate Resolution Imaging Spectrometer (MODIS) and the European Space Agency Along Track Scanning Radiometer (ATSR) and Advanced Along Track Scanning Radiometer (AATSR) may provide a useful augmentation to the record of gas flaring activity. The MODIS fire detection record extends from 2000 to 2007 and ancillary files exist tracking the records of coverages and cloud-free coverages. The ATSR active fire detection record extends back to 1995 could be produced and integrated into the identification of gas flares and the estimation of gas flaring volumes. The ATSR fire detection records extend from 1995 to 2007. Maximizing the value of the ATSR, AATSR and MODIS fire detections would require that the detection frequency be normalized to account for the number of valid observations.

Satellite detection of venting: Since 2005 more than a third of the countries examined show declines in natural gas flaring. In many cases the decline is not linked to declines in crude oil production indicating that the declines in flaring are due to changes in the handling of the associated gas. This could include improvements in the utilization of associated gas, increased reinjection, or increased venting. Because methane is twenty times stronger than CO₂ in terms of its greenhouse gas rating, venting is much worse than flaring. Having satellite observations capable of detecting and tracking venting would be a substantial complement to the direct detection of flaring. To date there have been several satellite instruments flown that had some capability to measure atmospheric pollutant concentrations at coarse spatial resolution (e.g., MOPITT and OMI Ozone Monitoring Instrument). The detection of methane releases associated with the venting of associated gas would require higher spatial resolution and an ability to resolve surface emissions from the large and seasonally variable background concentrations in other levels of the atmosphere.

This study indicates that satellite data can be used to estimate gas flaring volumes so that progress towards reductions can be identified and recognized. It is anticipated that by providing independent estimates of gas flaring volumes, satellite observations will play a key role in guiding efforts to reduce gas flaring. In many cases national governments responsible for establishing the regulatory framework for resource extraction have not known the magnitude of the flaring. Companies engaged in building the infrastructure to use or market associated gas may be able to use the results to identify gas flaring areas where their services may be offered. International petroleum companies will be able to assess the efficacy of efforts made to reduce gas flaring in remote locations under the direction of their subsidiaries and contractors. The satellite remote sensing of gas flares has moved from a curiosity to an operational and vital capability in the effort to reduce and ultimately eliminate most gas flaring.

Acknowledgements

This study was funded by the World Bank Global Gas Flaring Reduction (GGFR) initiative. Work by Dee W. Pack was funded by The Aerospace Corporation's Independent Research and Development program.

References and Notes

1. Croft, T.A. Burning waste gas in oil fields. *Nature* **1973**, *245*, 375–376.
2. Elvidge, C.D.; Baugh, K.E.; Kihn, E.A.; Kroehl, H.W.; Davis, E.R. Mapping city lights with nighttime data from the DMSP Operational Linescan System. *Photogramm. Eng. Remote Sensing* **1997**, *63*, 727–734.
3. Elvidge, C.D.; Imhoff, M.L.; Baugh, K.E.; Hobson, V.R.; Nelson, I.; Safran, J.; Dietz, J.B.; Tuttle, B.T. Night-time lights of the world: 1994–1995. *ISPRS J. Photogramm.* **2001**, *56*, 81–99.
4. Dobson, J.; Bright, E.A.; Coleman, P.R.; Durfee, R.C.; Worley, B.A. LandScan: a global population database for estimating populations at risk. *Photogramm. Eng. Remote Sensing* **2000**, *66*, 849–857.
5. *Energy Information Administration homepage*; Available online: <http://www.eia.doe.gov> (accessed August 4, 2009).
6. Elvidge, C.D.; Cinzano, P.; Pettit, D.R.; Arvesen, J.; Sutton, P.; Small, C.; Nemani, R.; Longcore, T.; Rich, C.; Safran, J.; Weeks, J.; Ebener, S. The Nightsat mission concept. *Int. J. Remote Sens.* **2007**, *28*, 2645–2670.

© 2009 by the authors; licensee Molecular Diversity Preservation International, Basel, Switzerland. This article is an open-access article distributed under the terms and conditions of the Creative Commons Attribution license (<http://creativecommons.org/licenses/by/3.0/>).